

TopoPoint: Enhance Topology Reasoning via Endpoint Detection in Autonomous Driving

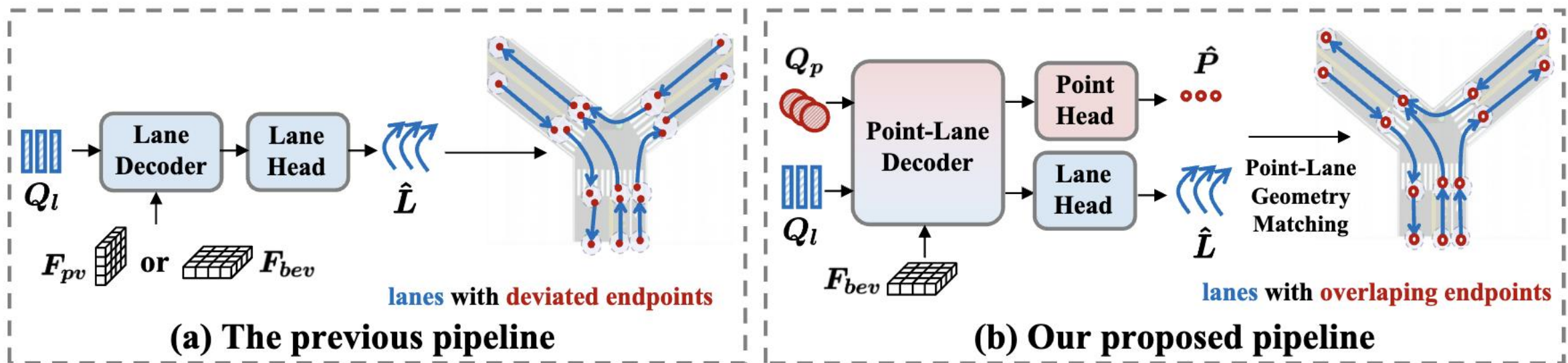
Yanping Fu^{1,2,3}, Xinyuan Liu^{1,2}, Tianyu Liu^{3,4}, Yike Ma¹, Yucheng Zhang¹, Feng Dai^{1*}

¹Institute of Computing Technology, Chinese Academy of Science;
²University of Chinese Academy of Sciences; ³Shanghai AI Lab; ⁴Shanghai Innovation Institute

fuyanping23s@ict.ac.cn

Motivation

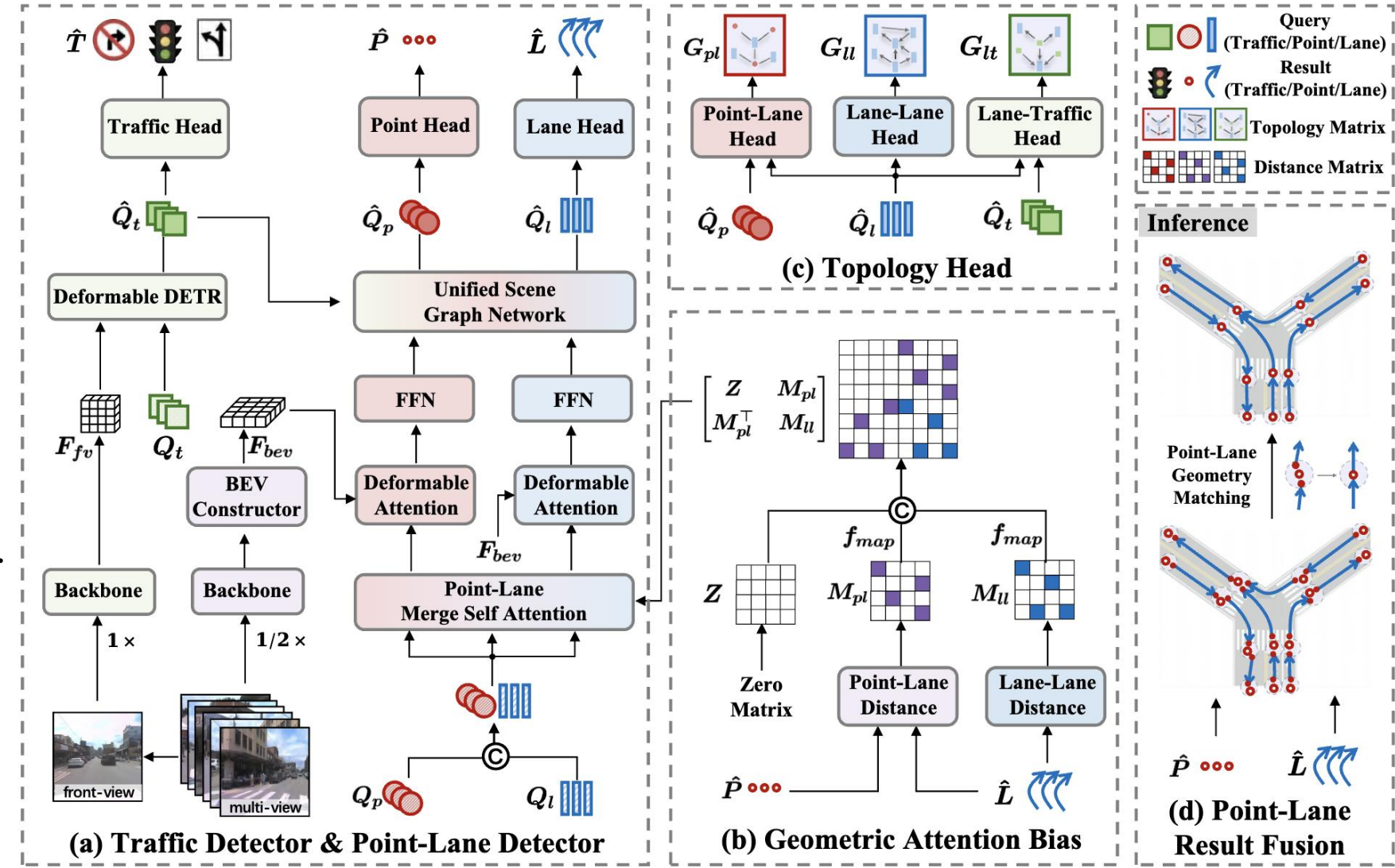
- In the previous pipeline, lanes are predicted independently, which leads to obvious endpoint deviation.
- In our proposed pipeline, lane endpoints are explicitly modeled, and lanes with overlapping endpoints are obtained through point-lane geometry matching.



Overview

- Traffic Detector
- Point-Lane Detector
- Topology Head
- Geometric Attention
- Point-Lane Fusion

- The multi-view images are downsampled by a factor of 0.5, while keeping the front-view at its original resolution.
- All images are passed through ResNet50 with FPN. The features are then encoded into BEV representations using BevFormer encoder.



Pipeline

- **Traffic Detector:** In the traffic detector, front-view features are directly processed by Deformable DETR to produce traffic query.

$$\begin{aligned}\hat{Q}_t &= \text{DeformableDETR}(Q_t, F_{fv}) \\ \hat{T} &= \text{TrafficHead}(\hat{Q}_t)\end{aligned}$$

- **Point-Lane Detector:** In the point-lane detector, point query and lane query interact via *Point-Lane Merge Self-Attention*, which computes geometric attention bias serving as an attention mask to enhance global information sharing. The resulting queries then perform cross-attention with BEV features. Then all queries are fed into *Unified Scene Graph Network*.

$$Q_{pl} = \text{Concat}(Q_p, Q_l)$$

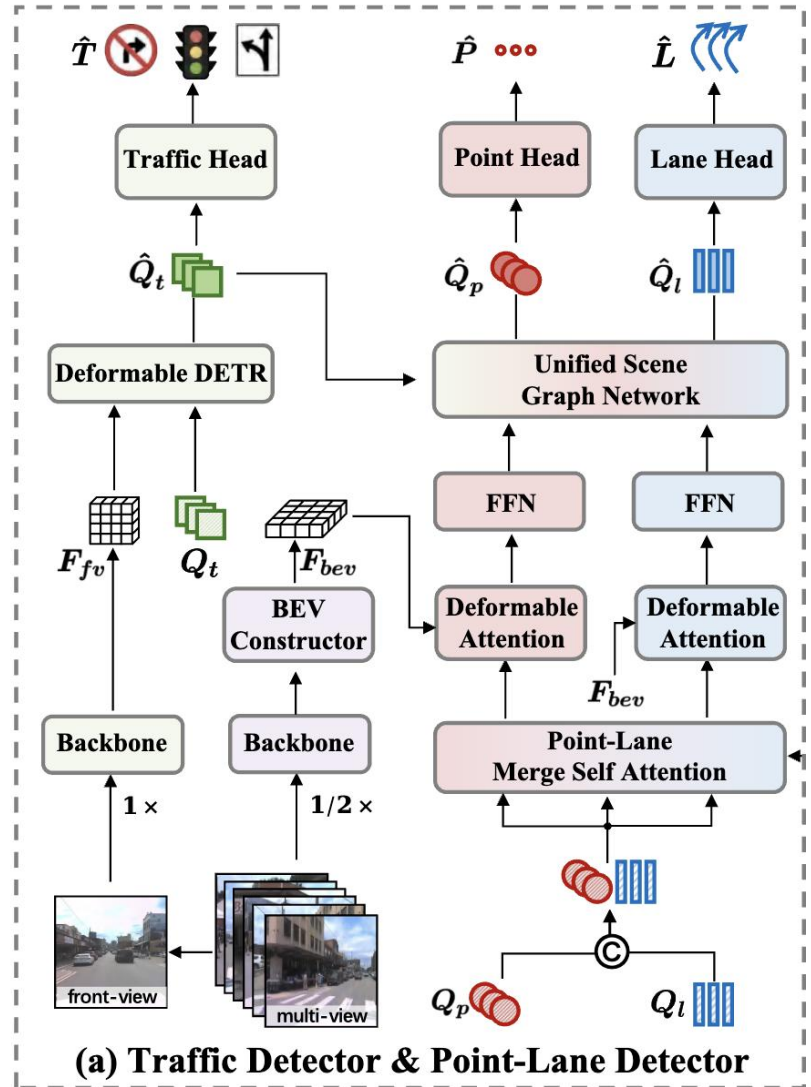
$$Q_p, Q_l = \text{PointLaneMergeSelfAttention}(Q_{pl})$$

$$Q_p, Q_l = \text{LN}(\text{DeformAttn}(Q_p, R_p, F_{bev})), \text{LN}(\text{DeformAttn}(Q_l, R_l, F_{bev}))$$

$$Q_p, Q_l = \text{LN}(\text{FFN}(Q_p)), \text{LN}(\text{FFN}(Q_l))$$

$$Q_p, Q_l = \text{UnifiedSceneGraphNetwork}(Q_p, Q_l, \hat{Q}_t)$$

$$\hat{P} = \text{PointHead}(\hat{Q}_p), \hat{L} = \text{LaneHead}(\hat{Q}_l)$$



Pipeline

- **Point-Lane Attention:** The geometric attention bias is also incorporated into the point-lane merge self attention module to exchange information.
- To incorporate the geometric relationships between points and lanes in the BEV space, we compute their pairwise geometric distances based on the predicted points and lanes from the previous decoder layer
- To compute self-attention, we concatenate distance matrixes to form geometric attention bias, which is added to the attention weights computed from original queries.

$$Q_{pl} = \text{Concat}(Q_p, Q_l)$$

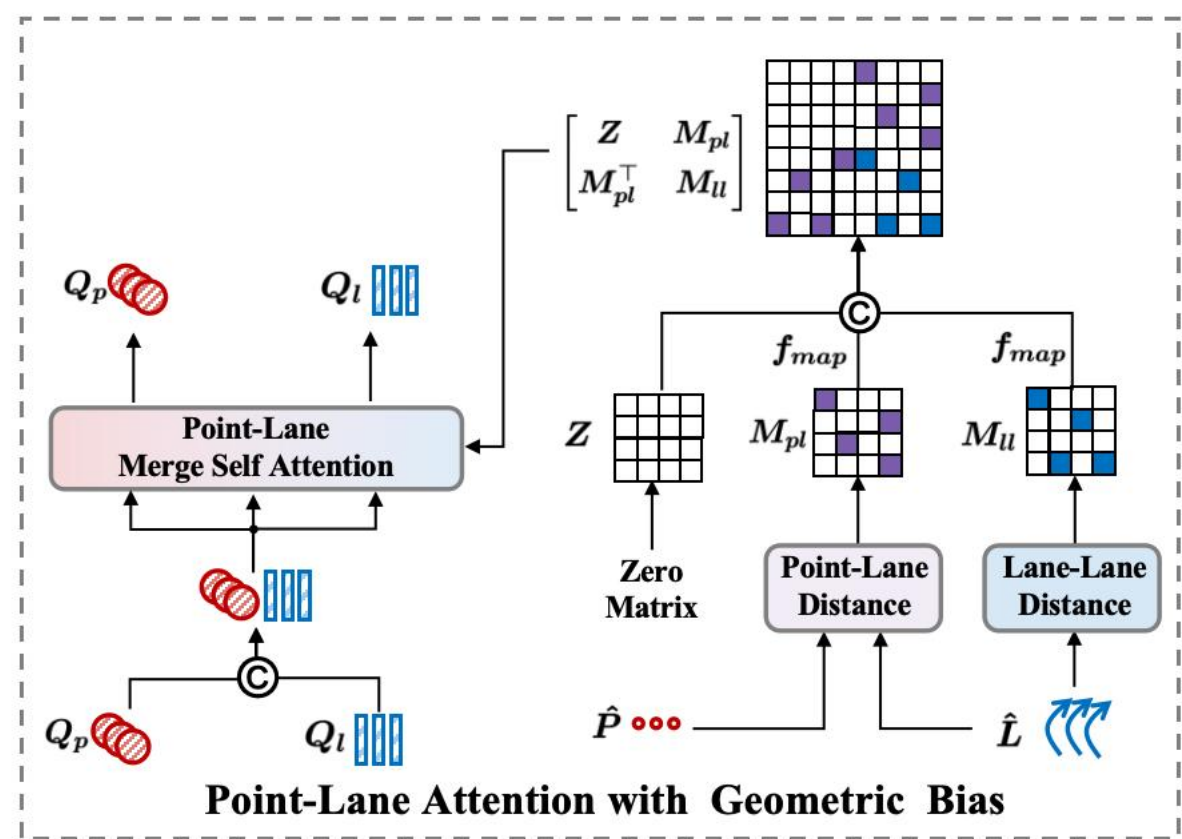
$$D_{ll} = \left\{ \sum |\hat{l}_i^e - \hat{l}_j^s| \mid i = 1, 2, \dots, N_p, j = 1, 2, \dots, N_l \right\}$$

$$D_{pl} = \left\{ \min \left(\sum |\hat{p}_i - \hat{l}_j^s|, \sum |\hat{p}_i - \hat{l}_j^e| \right) \mid i = 1, 2, \dots, N_p, j = 1, 2, \dots, N_l \right\}$$

$$M_{pl} = f_{map}(D_{pl}), M_{ll} = f_{map}(D_{ll})$$

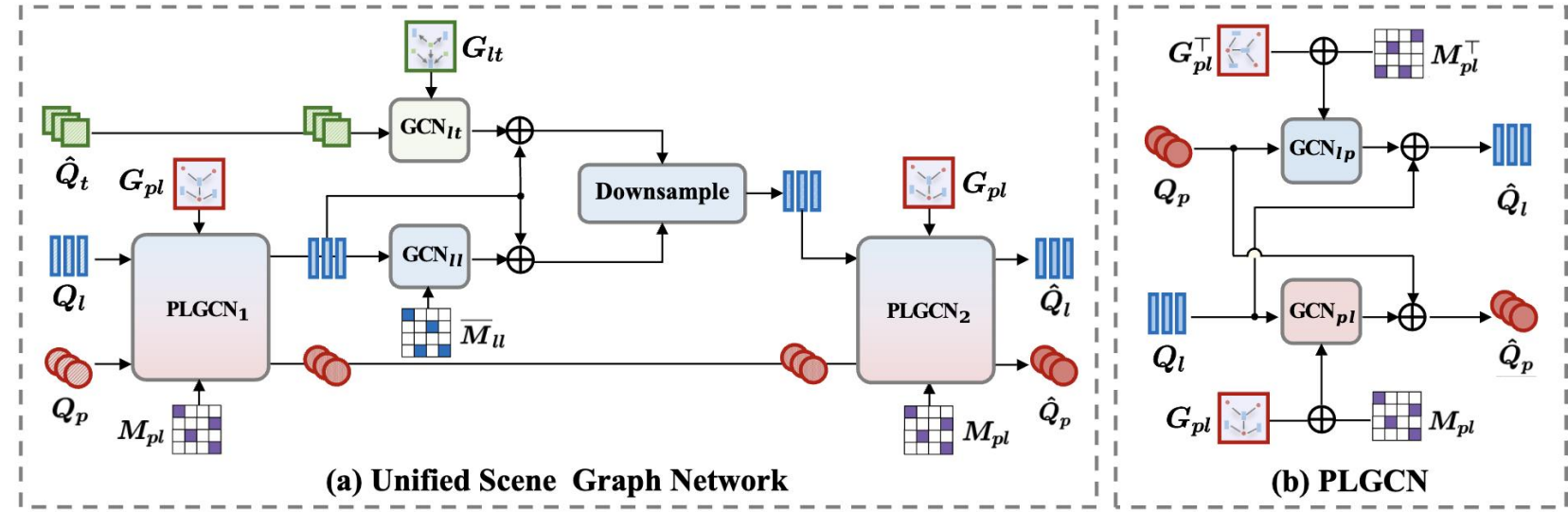
$$Q_p, Q_l = \text{Softmax} \left(\frac{Q_{pl} \cdot Q_{pl}^\top}{\sqrt{d}} + \begin{bmatrix} Z & M_{pl} \\ M_{pl}^\top & M_{ll} \end{bmatrix} \right) \cdot Q_{pl}$$

$$Q_p, Q_l = \text{LN}(Q_p), \text{LN}(Q_l)$$



Pipeline

- **Unified Scene Graph Network:** Based on geometric attention bias and reasoned topology, lane & point queries are enhanced from the associated traffic elements & lanes & points by the unified scene graph network.
- **PLGCN:** The submodule is designed to facilitate bidirectional feature aggregation between point and lane based on their geometric relationships.



$$\begin{aligned}
 A_{pl} &= \lambda_1 G_{pl} + \lambda_2 M_{pl} \\
 Q_p &= \text{GCN}_{pl}(Q_l, A_{pl}) + Q_p, \quad Q_l = \text{GCN}_{lp}(Q_p, A_{pl}^\top) + Q_l \\
 Q_p^1, Q_l^1 &= \text{PLGCN}_1(Q_p, Q_l, M_{pl}, G_{pl}) \\
 Q_l^2 &= \text{Downsample} \left(\text{Concat} \left(\text{GCN}_{ll}(Q_l^1, \bar{M}_{ll}) + Q_l^1, \text{GCN}_{lt}(\hat{Q}_t, G_{lt}) + Q_l^1 \right) \right) \\
 Q_p^3, Q_l^3 &= \text{PLGCN}_2(Q_p^1, Q_l^2, M_{pl}, G_{pl}) \\
 \hat{Q}_p, \hat{Q}_l &= Q_p^3, Q_l^3
 \end{aligned}$$

Pipeline

- **Topology Head** : The queries are used for topology reasoning, and the topology is also used for query enhancement in scene graph.

$$\hat{G}_{pl} = \text{Sigmoid}(\text{MLP}(\hat{Q}_p) \cdot \text{MLP}(\hat{Q}_l)^\top)$$

$$\hat{G}_{ll} = \text{Sigmoid}(\text{MLP}(\hat{Q}_l) \cdot \text{MLP}(\hat{Q}_l)^\top)$$

$$\hat{G}_{lt} = \text{Sigmoid}(\text{MLP}(\hat{Q}_l) \cdot \text{MLP}(\hat{Q}_t)^\top)$$

- **PointLane Geometry Matching Algorithm:**

During inference, predicted points and lanes are fused via Point-Lane Geometry Matching algorithm to refine lane endpoints and effectively mitigate the endpoint deviation problem.

Algorithm 1: Point-Lane Geometry Matching Algorithm

Input: Predicted points $\hat{P}_{reg}, \hat{P}_{cls}$; predicted lanes $\hat{L}_{reg}, \hat{L}_{cls}$; classification thresholds τ_p, τ_l ; geometry distance threshold δ .

Output: Refined lanes \hat{L}_{ref}

Step 1: High-Confidence Filtering

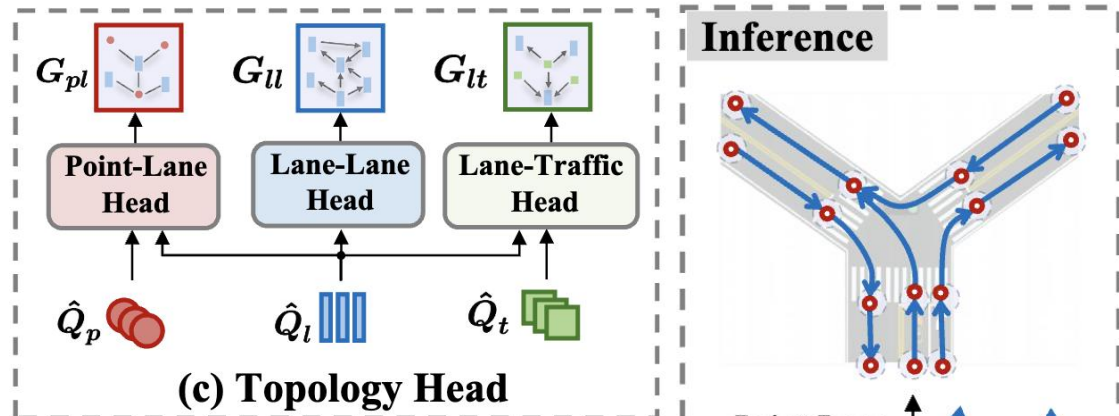
Filter points with high classification scores: $\hat{P}_{select} = \{\hat{P}_{reg}^i \mid \hat{P}_{cls}^i > \tau_p\}$

Filter lanes with high classification scores: $\hat{L}_{select} = \{\hat{L}_{reg}^j \mid \hat{L}_{cls}^j > \tau_l\}$

Step 2: Geometry-Based Matching and Refinement

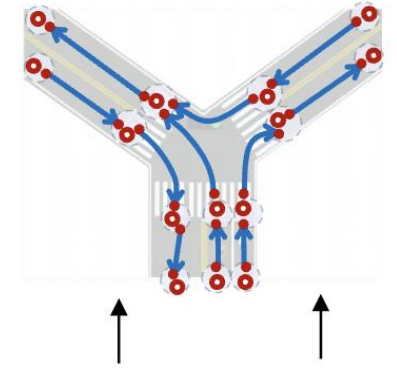
```

foreach point  $\hat{P}_i \in \hat{P}_{select}$  do
    Initialize empty match set:  $\mathcal{N}_i = \emptyset$  ;
    foreach lane  $\hat{L}_j \in \hat{L}_{select}$  do
        if  $distance(\hat{P}_i, \hat{L}_j^{endpoint}) < \delta$  then
            Add  $\hat{L}_j$  to  $\mathcal{N}_i$  ;
    if  $\mathcal{N}_i \neq \emptyset$  then
        Compute refined endpoint:
         $\hat{E}_i = \frac{1}{|\mathcal{N}_i|+1} (\hat{P}_i + \sum_{\hat{L}_j \in \mathcal{N}_i} \hat{L}_j^{endpoint})$ ;
        Update endpoints of all  $\hat{L}_j \in \mathcal{N}_i$  with  $\hat{E}_i$ ;
return  $\hat{L}_{ref}$  with refined endpoints
    
```



Inference

Point-Lane Geometry Matching



(d) Point-Lane Result Fusion

Experiments Setup

- **Dataset:** OpenLaneV2, which is constructed based on Argoverse2 and nuScenes. OpenLane-V2 is divided into two subsets: subset_A and subset_B, each containing 1,000 scenes captured at 2 Hz with multi-view images and corresponding annotations.
- **Metric:** We adopt the evaluation metrics defined by OpenLane-V2, including DET_l, DET_t, TOP_{ll}, and TOP_{lt}, all of which are computed based on mean Average Precision (mAP)

$$\text{OLS} = \frac{1}{4} [\text{DET}_l + \text{DET}_t + \sqrt{\text{TOP}_{ll}} + \sqrt{\text{TOP}_{lt}}]$$

- **Point Metric:** In addition, to evaluate the performance of endpoint detection, we define a custom metric DET_p, which is computed as the average over match thresholds $T = \{1.0, 2.0, 3.0\}$ based on the point-wise Fréchet distance, as follows:

$$\text{DET}_p = \frac{1}{|\mathbb{T}|} \sum_{t \in \mathbb{T}} AP_t$$

Main Results

■ Comparison on OpenLane-v2 Benchmark: New SOTA results and more precise endpoints.

Data	Method	Conference	$\text{DET}_l \uparrow$	$\text{DET}_t \uparrow$	$\text{TOP}_{ll} \uparrow$	$\text{TOP}_{lt} \uparrow$	$\text{OLS} \uparrow$	$\text{DET}_p \uparrow$
subset_A	STSU[13]	ICCV2021	12.7	43.0	2.9	19.8	29.3	-
	VectorMapNet[10]	ICML2023	11.1	41.7	2.7	9.2	24.9	-
	MapTR[48]	ICLR2023	17.7	43.5	5.9	15.1	31.0	-
	TopoNet[26]	Arxiv2023	28.6	48.6	10.9	23.8	39.8	43.8
	TopoMLP[29]	ICLR2024	28.3	49.5	21.6	26.9	44.1	43.4
	TopoLogic[15]	NeurIPS2024	29.9	47.2	23.9	25.4	44.1	45.2
	TopoFormer*[31]	CVPR2025	34.7	48.2	24.1	29.5	46.3	-
	TopoPoint (Ours)	-	31.4	55.3	28.7	30.0	48.8	52.6
subset_B	STSU[13]	ICCV2021	8.2	43.9	-	-	-	-
	VectorMapNet[10]	ICML2023	3.5	49.1	-	-	-	-
	MapTR[48]	ICLR2023	15.2	54.0	-	-	-	-
	TopoNet[26]	Arxiv2023	24.3	55.0	6.7	16.7	36.8	38.5
	TopoMLP[29]	ICLR2024	26.6	58.3	21.0	19.8	43.8	39.6
	TopoLogic[15]	NeurIPS2024	25.9	54.7	21.6	17.9	42.3	39.2
	TopoFormer*[31]	CVPR2025	34.8	58.9	23.2	23.3	47.5	-
	TopoPoint (Ours)	-	31.2	60.2	28.3	27.1	49.2	45.1

Ablation Studies

■ Impact of each module:

Module	$\text{DET}_l \uparrow$	$\text{DET}_t \uparrow$	$\text{TOP}_{ll} \uparrow$	$\text{TOP}_{lt} \uparrow$	$\text{OLS} \uparrow$	$\text{DET}_p \uparrow$
Baseline	29.2	46.8	23.4	24.3	43.4	44.5
+ FVScale	29.4	53.8	23.8	27.0	46.0	44.8
+ PLMSA	30.2	54.8	27.2	28.5	47.6	49.8
+ PLGCN	30.8	55.3	28.0	29.2	48.3	51.8
+ PLGM	31.4	55.3	28.7	30.0	48.8	52.6

■ Effect of different GCNs:

Module	$\text{DET}_l \uparrow$	$\text{DET}_t \uparrow$	$\text{TOP}_{ll} \uparrow$	$\text{TOP}_{lt} \uparrow$	$\text{OLS} \uparrow$	$\text{DET}_p \uparrow$
w/o GCN	28.9	53.9	25.6	26.4	46.2	48.6
+ GCN_{ll}	29.8	54.2	26.9	27.1	47.0	49.8
+ GCN_{lt}	30.6	54.5	27.4	28.8	47.8	50.5
+ PLGCN_1	30.9	55.0	28.2	29.5	48.3	51.9
+ PLGCN_2	31.4	55.3	28.7	30.0	48.8	52.6

Ablation Studies

■ Image scales set up:

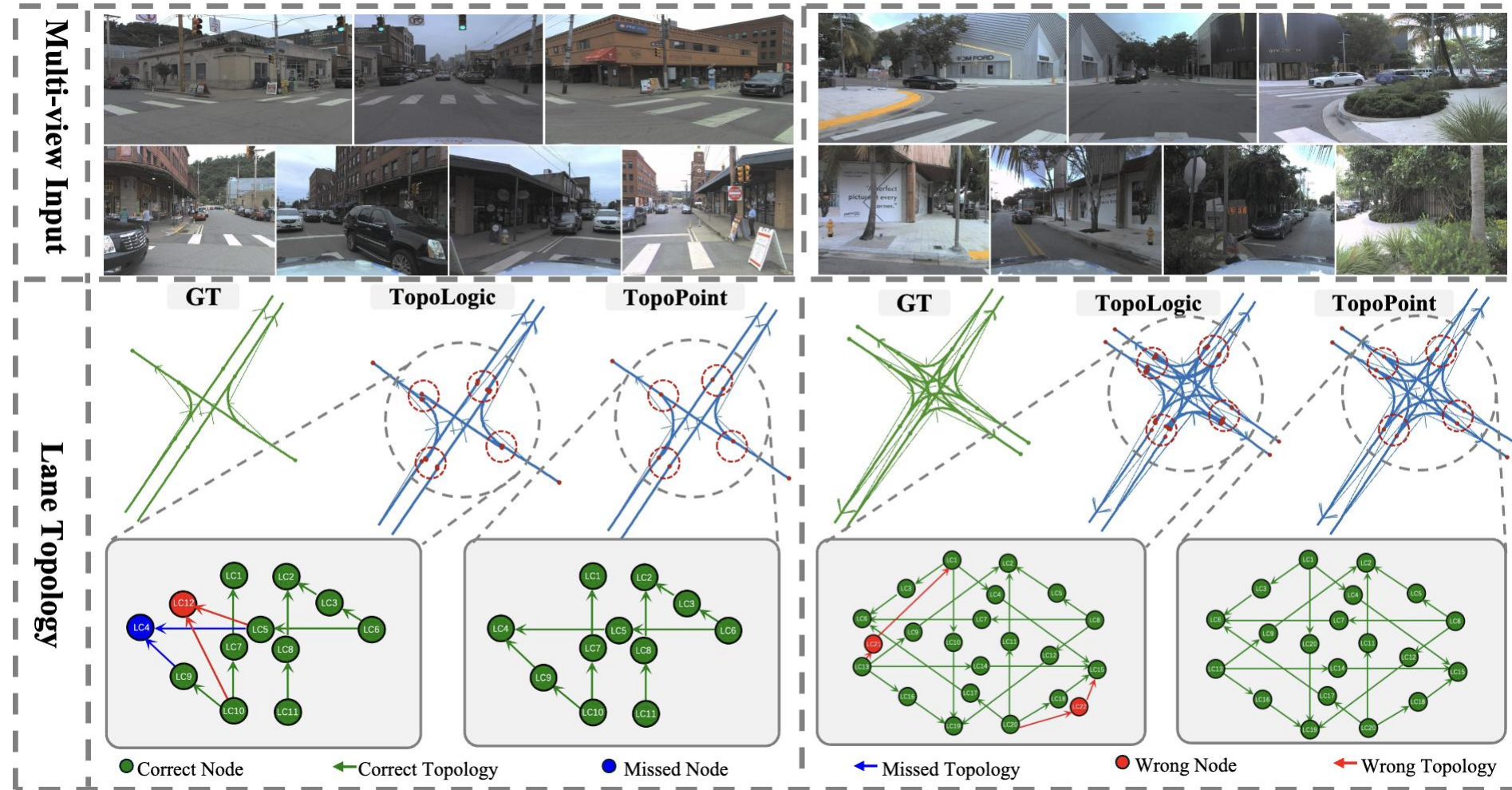
S_{fv}	S_{mv}	DET _l ↑	DET _t ↑	TOP _{ll} ↑	TOP _{lt} ↑	OLS↑	DET _p ↑
0.5	0.5	31.2	48.6	28.5	28.4	46.6	52.3
0.5	1.0	30.5	48.3	28.0	27.9	46.1	51.5
1.0	0.5	31.4	55.3	28.7	30.0	48.8	52.6
1.0	1.0	30.8	54.7	28.3	28.9	48.1	51.8

■ Effect of point and lane query numbers:

N_p	N_l	DET _l ↑	DET _t ↑	TOP _{ll} ↑	TOP _{lt} ↑	OLS↑	DET _p ↑
100	200	29.5	54.3	25.6	27.0	46.5	49.7
200	200	30.7	53.7	27.4	28.2	47.5	51.8
200	300	31.4	55.3	28.7	30.0	48.8	52.6
300	300	30.8	54.6	28.2	29.8	48.3	51.4

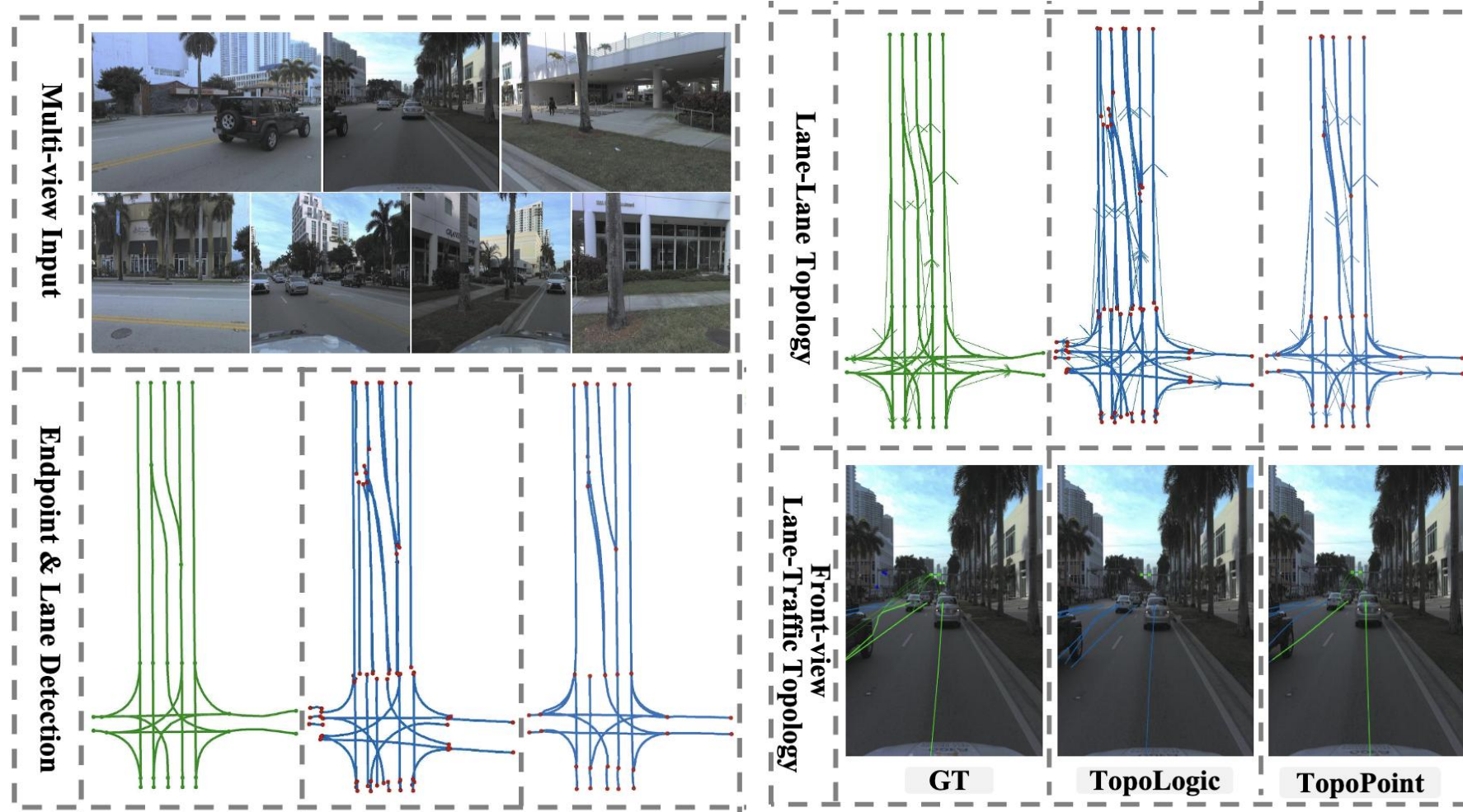
Qualitative Analysis

■ Comparison of TopoLogic and our TopoPoint:



Qualitative Analysis

■ Comparison of TopoLogic and our TopoPoint:





THANK YOU!